

## ON THE DISTRIBUTION OF CURRENT ON AN OPEN TAPE HELIX

N. Kalyanasundaram, G. Naveen Babu, and R. Tulsian

Jaypee Institute of Information Technology  
A-10, Sector-62, Noida-201307, India

**Abstract**—The approximate distribution of the current density induced on the tape surface by guided electromagnetic waves supported by an infinite open tape helix is estimated from an exact solution of a homogenous boundary value problem for Maxwell's equations. It is shown that the magnitude of the surface current density component perpendicular to the winding direction is at least three orders of magnitude smaller than that of the surface current density component parallel to the winding direction everywhere on the tape surface. Also, the magnitude and phase distribution for the surface current density components parallel and perpendicular to the winding direction are seen to be nearly uniform at all frequencies corresponding to real values of the propagation constant.

### 1. INTRODUCTION

Ever since the pioneering work of Samuel Sensiper on Electromagnetic Wave Propagation on Helical Conductors [1] until very recently, almost all the published derivations of the dispersion equation for electromagnetic waves guided by a tape helix [2–7] except that of Chernin et al. [8] involved an ad hoc assumption about the tape-current distribution. As a consequence, the tangential electric field boundary conditions on the tape surface could be satisfied only in some approximate sense. The necessity of such an ad hoc assumption on the tape-current distribution was due to the inherent inability of the series expansion for the tape-current density to correctly confine the surface current to the region of tape only. In other words, the infinite series for the tape-current density ought to have summed automatically to zero at any point in the gap region (the region on the surface of the infinite cylinder between the tapes).

---

Corresponding author: N. Kalyanasundaram (n.kalyanasundaram@jiit.ac.in).

All previous work on the tape-helix model except [8] has made use of the ‘narrow tape’ assumption which amounts to neglecting the component of the tape-current density perpendicular to the winding direction. Within the narrow-tape assumption, a variety of distributions for tape current has been proposed in the literature, the record being held by Zhang and Li who propose not less than six different models for tape-current distribution in their book [4]. Basu [5], on the other hand, restricts his analysis to the more popular model wherein the tape-current density parallel to the winding direction is assumed to have a constant amplitude over the tape width with a phase that varies in the winding direction according to the factor  $\exp(j\beta_0 z)$  where  $\beta_0$  is the propagation constant and the axial coordinate  $z$  corresponds to a point moving along the center line of the tape.

Although the derivation of the dispersion equation presented by Chernin et al. involves neither any a priori assumption about the tape-current distribution except for its behavior near the tape edges nor any approximations in satisfying the tangential electric field boundary conditions on the tape surface, their surface-current density expansions, which are assumed to have a form identical to those of the field components when restricted to the surface of the infinite cylinder containing the tape helix, do not again seem to be capable of limiting the support of the surface-current density to the region of the tape only. Moreover, reexpansions of the tape current density components in terms of Chebyshev polynomials resorted to by Chernin et al., seem to be motivated by the anticipated singularity of the surface current density component parallel to the winding direction near the tape edges. Such an a priori assumption regarding the edge behavior of the surface current density component is totally unnecessary as an ordinary Fourier-series expansion is pretty well capable of bringing out any such singular behavior, if present, as long as the singularity is integrable. Another anomalous behavior displayed by the surface-current density plots obtained by Chernin et al. concerns the lack of symmetry about the center line of the tape.

In this paper, amplitude and phase plots of the tape-current distribution following from the exact analysis developed in [9] are presented for a finite order of truncation of the Fourier-series representation of the tape-current density. The main conclusions that may be drawn are (i) the magnitude and the phase distribution of the surface current density components parallel and perpendicular to the winding direction are nearly uniform at all frequencies corresponding to the allowed portions of the dispersion curve even for tapes which are not narrow and (ii) the magnitude of the surface current density

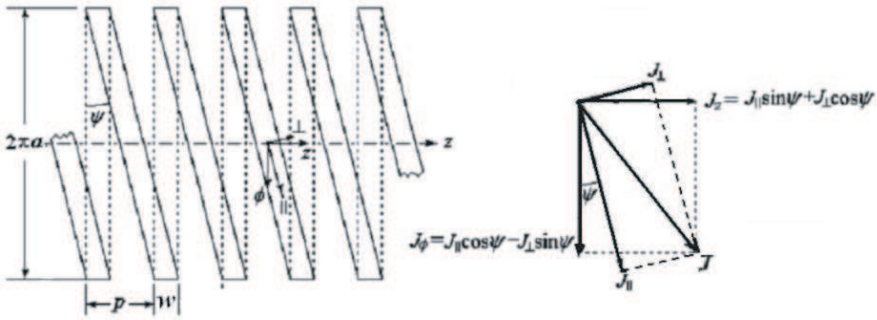


**Figure 1.** Geometrical relations and surface current density components in a developed tape helix.

component perpendicular to the winding direction is at least three orders of magnitude smaller than that of the surface current density component parallel to the winding direction everywhere on the tape surface.

**2. REVIEW OF BASIC THEORY**

We make use of the tape-helix model introduced in [9]. Accordingly, we consider a perfectly conducting tape helix of infinite length, constant pitch, constant tape width and infinitesimal thickness surrounded by free space. We take the axis of the helix along the  $z$ -coordinate of a cylindrical coordinate system  $(\rho, \varphi, z)$ . The radius of the helix is  $a$ , the pitch is  $p$ , and the width of the tape in the axial direction is  $w$ . The pitch angle  $\psi$  is therefore given by  $\cot \psi = 2\pi a/p$ .

We now briefly recall those aspects of the analysis presented in [9] that will have a direct bearing on the computation of the current distribution on the tape helix. The axial component  $J_z(z, \varphi)$  and the azimuthal component  $J_\varphi(z, \varphi)$  of the surface current density, which are confined only to the tape surface, admit the representations

$$\begin{aligned}
 J_m(z, \varphi) &= \tilde{J}_m(z, \zeta) = e^{-j\beta_0 z} f_m(\zeta) \\
 &= e^{-j\beta_0 z} \sum_{l=-\infty}^{\infty} 1_{[lp-w/2, lp+w/2]}(\zeta) \sum_{n=-\infty}^{\infty} J_{mn} e^{-j2\pi n\zeta/p}, \\
 & \qquad \qquad \qquad m = z, \varphi, \quad (1)
 \end{aligned}$$

where

$$\zeta = z - \varphi p/2\pi, \quad (2)$$

$\beta_0 = \beta_0(\omega)$  is the guided wave propagation constant at the radian frequency  $\omega$ , and for  $l \in \mathbb{Z}$

$$1_{[lp-w/2, lp+w/2]}(\zeta) \triangleq \begin{cases} 1 & \text{if } \zeta \in [lp - w/2, lp + w/2], \\ 0 & \text{if } \zeta \notin [lp - w/2, lp + w/2] \end{cases}$$

The (complex) constant coefficients  $J_{zn}$  and  $J_{\varphi n}$ ,  $n \in \mathbb{Z}$ , appearing in the expansion (1) of the surface current density components are determined (in terms of any one of the constants  $J_{z0}$  and  $J_{\varphi 0}$ ) by the tape-helix boundary conditions. The enforcement of these boundary conditions lead to two infinite sets of linear homogeneous equations for determining the two infinite sets of coefficients  $J_{zq}$  and  $J_{\varphi q}$ ,  $q \in \mathbb{Z}$ :

$$\mathbf{A}_\mu \mathbf{J}_z - \mathbf{A}_\nu \mathbf{J}_\varphi = \mathbf{0} \quad (3a)$$

$$\mathbf{A}_\nu \mathbf{J}_z - \mathbf{A}_\eta \mathbf{J}_\varphi = \mathbf{0} \quad (3b)$$

where  $\mathbf{0}$  denotes the column vector of infinite number of zeros. In (3)

$$\mathbf{J}_m = [\dots, J_{m\bar{2}}, J_{m\bar{1}}, J_{m0}, J_{m1}, J_{m2}, \dots]^T, \quad m = z, \varphi$$

where  $\bar{n} \triangleq -n$  for  $n \in \mathbb{Z}/\{0\}$  and

$$\mathbf{A}_\mu = [\mu_{kq}]_{k,q \in \mathbb{Z}}, \quad \mathbf{A}_\nu = [\nu_{kq}]_{k,q \in \mathbb{Z}} \quad \text{and} \quad \mathbf{A}_\eta = [\eta_{kq}]_{k,q \in \mathbb{Z}}$$

are infinite-order matrices with entries

$$\mu_{kq} = \sum_{n=-\infty}^{\infty} \mu_n \text{sinc}(k-n) \hat{w} \text{sinc}(q-n) \hat{w} \quad (4a)$$

$$\nu_{kq} = \sum_{n=-\infty}^{\infty} \nu_n \text{sinc}(k-n) \hat{w} \text{sinc}(q-n) \hat{w} \quad (4b)$$

$$\eta_{kq} = \sum_{n=-\infty}^{\infty} \eta_n \text{sinc}(k-n) \hat{w} \text{sinc}(q-n) \hat{w} \quad (4c)$$

where

$$\mu_n \triangleq \tau_{na}^2 I_{na} K_{na} \quad (5a)$$

$$\nu_n \triangleq n \beta_{na} I_{na} K_{na} \quad (5b)$$

$$\eta_n \triangleq k_{0a}^2 I'_{na} K'_{na} + (n \beta_{na} / \tau_{na})^2 I_{na} K_{na} \quad (5c)$$

and  $\hat{w} \triangleq w/p$ . In (5)

$$k_{0a} \triangleq ak_0 = a\omega \sqrt{\mu\epsilon},$$

$$\beta_{0a} = a\beta_0,$$

$$\beta_{na} = \beta_{0a} + n \cot \psi,$$

$$\tau_{na}^2 = \beta_{na}^2 - k_{0a}^2$$

and we have used the following abbreviations

$$I_{na} \triangleq I_n(\tau_{na}),$$

$$K_{na} \triangleq K_n(\tau_{na}),$$

$$I'_{na} \triangleq I'_n(\tau_{na}), \quad K'_{na} \triangleq K'_n(\tau_{na}),$$

for the modified Bessel functions and their derivatives evaluated at  $\rho = a$ . Solving (3a) for  $\mathbf{J}_\varphi$  in terms of  $\mathbf{J}_z$  as

$$\mathbf{J}_\varphi = \mathbf{A}_\nu^{-1} \mathbf{A}_\mu \mathbf{J}_z \tag{6}$$

and substituting into (3b), we have the infinite set of equations

$$[\mathbf{A}_\nu - \mathbf{A}_\eta \mathbf{A}_\nu^{-1} \mathbf{A}_\mu] \mathbf{J}_z = \mathbf{0} \tag{7}$$

for determining the infinite set of coefficients  $J_{zq}$ ,  $q \in \mathbb{Z}$ . For a nontrivial solution for  $\mathbf{J}_z$ , it is necessary that

$$|\mathbf{A}_\nu - \mathbf{A}_\eta \mathbf{A}_\nu^{-1} \mathbf{A}_\mu| = 0 \tag{8}$$

The determinantal condition (8) gives, in principle, the dispersion equation for the cold-wave modes supported by an open perfectly conducting infinite tape helix of infinitesimal thickness and finite width.

### 3. NUMERICAL COMPUTATION OF THE TAPE-CURRENT DISTRIBUTION

As in [9], the infinite-order matrices  $\mathbf{A}_\mu$ ,  $\mathbf{A}_\nu$  and  $\mathbf{A}_\eta$  are symmetrically truncated to  $(2N + 1) \times (2N + 1)$  matrices  $\hat{\mathbf{A}}_\mu$ ,  $\hat{\mathbf{A}}_\nu$  and  $\hat{\mathbf{A}}_\eta$ . It is readily seen from (4a)–(4c) that only the main lobes of the *sinc* functions contribute significantly to the values of  $\mu_{kq}$ ,  $\nu_{kq}$  and  $\eta_{kq}$ ,  $k, q \in \mathbb{Z}$ . Thus, for the choice of axial width-to-pitch ratio  $\hat{w} = 1/2$ , the infinite-series for them get truncated to [9]

$$b_{kq} \triangleq \hat{\mu}_{kq} = \sum_{n=\max(k,q)-1}^{\min(k,q)+1} \mu_n \text{sinc}\left(\frac{k-n}{2}\right) \text{sinc}\left(\frac{q-n}{2}\right) \tag{9a}$$

$$c_{kq} \triangleq \hat{\nu}_{kq} = \sum_{n=\max(k,q)-1}^{\min(k,q)+1} \nu_n \text{sinc}\left(\frac{k-n}{2}\right) \text{sinc}\left(\frac{q-n}{2}\right) \tag{9b}$$

$$d_{kq} \triangleq \hat{\eta}_{kq} = \sum_{n=\max(k,q)-1}^{\min(k,q)+1} \eta_n \text{sinc}\left(\frac{k-n}{2}\right) \text{sinc}\left(\frac{q-n}{2}\right) \tag{9c}$$

**Remark:** Unlike the  $\sigma_n$  of [10] that decay asymptotically with respect to  $|n|$ , the  $\mu_n$ ,  $\nu_n$  and  $\eta_n$  appearing in (5) exhibit an asymptotic growth with respect to  $|n|$ . Hence, the contributions to the values of  $\mu_{kq}$ ,  $\nu_{kq}$  and  $\eta_{kq}$ ,  $k, q \in \mathbb{Z}$ , from the side lobes of the sinc functions may not be as insignificant as would have been the case had the asymptotic

behavior of  $\mu_n, \nu_n$  and  $\eta_n$  been the same as that of  $\sigma_n$  with respect to  $|n|$ .

When the contributions from the main lobes of the sinc functions only are retained in the expressions for  $b_{kq}, c_{kq}$  and  $d_{kq}$ ,  $-N \leq k, q \leq N$ , there will only be three types of non-zero entries in the  $(2N+1) \times (2N+1)$  symmetric matrices  $\hat{\mathbf{A}}_\mu, \hat{\mathbf{A}}_\nu$  and  $\hat{\mathbf{A}}_\eta$  for the choice  $\hat{w} = 1/2$ , viz.,

$$\begin{aligned} b_{k,k} &= \mu_k + (2/\pi)^2(\mu_{k-1} + \mu_{k+1}) & -N \leq k \leq N, \\ b_{k,k+1} &= b_{k+1,k} = (2/\pi)(\mu_k + \mu_{k+1}) & -N \leq k \leq N-1, \\ b_{k,k+2} &= b_{k+2,k} = (2/\pi)^2\mu_{k+1} & -N \leq k \leq N-2 \end{aligned}$$

with similar relations for  $c_{k,k+i}$  and  $d_{k,k+i}$ ,  $i = 0, 1, 2$ . Thus, the truncated coefficient matrices  $\hat{\mathbf{A}}_\mu, \hat{\mathbf{A}}_\nu$  and  $\hat{\mathbf{A}}_\eta$  will be banded symmetric matrices with nonzero entries only along the main diagonal and the four symmetrically located subdiagonals adjacent to the main diagonal. Thus, the approximate dispersion equation corresponding to a truncation order equal to  $N$  becomes

$$\left| \hat{\mathbf{A}}_\nu - \hat{\mathbf{A}}_\eta \hat{\mathbf{A}}_\nu^{-1} \hat{\mathbf{A}}_\mu \right| = 0 \quad (10)$$

Exhaustive numerical simulation of (10) to find a real root  $\hat{k}_{0a}(\beta_{0a})$  of the approximate dispersion equation for  $k_{0a}$  as a function of  $\beta_{0a}$  carried out in [9] for various truncation orders reveals that a truncation order of  $N = 3$  is adequate to deliver a fairly accurate estimate of  $\hat{k}_{0a}(\beta_{0a})$  for the parameter value of  $\hat{w} = 1/2$  and  $\psi = 10^\circ$ .

Although a truncation order as low as  $N = 3$  was found to be adequate for securing an accurate estimate for  $\hat{k}_{0a}(\beta_{0a})$ , fairly large number  $N$  of the ‘current density coefficients’  $\hat{J}_{zn}$  and  $\hat{J}_{\varphi n}$ ,  $0 \leq |n| \leq N$ , corresponding to  $\hat{\beta}_{0a}(k_{0a})$  (where  $\hat{\beta}_{0a}(k_{0a})$  is the estimate of the normalized propagation constant corresponding to the normalized frequency  $k_{0a}$ , that is, the unique root of the equation  $\hat{k}_{0a}(\beta_{0a}) = k_{0a}$  for  $\beta_{0a}$ ) are needed in the series representation (1) of the surface current density components  $J_z(z, \varphi)$  and  $J_\varphi(z, \varphi)$  in order to be assured of a reasonably good approximation for the tape-current density.

Stacking the first  $(2N+1)$  (for  $N$  large enough) lowest order coefficients in the expansion (1) of the surface current density components into the two  $(2N+1)$ -dimensional vectors  $\hat{\mathbf{J}}_m = \left[ \hat{J}_{mN}, \hat{J}_{m(N-1)}, \dots, \hat{J}_{m1}, \hat{J}_{m0}, \hat{J}_{m1}, \dots, \hat{J}_{m(N-1)}, \hat{J}_{mN} \right]^T$ ,  $m = z, \varphi$ , the truncated versions of (6) and (7) may be expressed as

$$\hat{\mathbf{J}}_\varphi = \hat{\mathbf{A}}_\nu^{-1} \hat{\mathbf{A}}_\mu \hat{\mathbf{J}}_z \quad (11)$$

and

$$\left[ \hat{\mathbf{A}}_\nu - \hat{\mathbf{A}}_\eta \hat{\mathbf{A}}_\nu^{-1} \hat{\mathbf{A}}_\mu \right] \hat{\mathbf{J}}_z = \mathbf{0} \quad (12)$$

where  $\mathbf{0}$  denotes the column vector of  $(2N + 1)$  zeros. Thus, the task before us is to find the null-space vector of a  $(2N + 1) \times (2N + 1)$  ( $N$  large) rank-deficient matrix corresponding the the already located root  $\hat{k}_{0a}(\beta_{0a})$  of the determinantal Equation (10). A direct method of doing this is likely to be computationally very intensive because of the large size of the coefficient matrix in (12). Fortunately, an alternative computationally more efficient method for iteratively computing the null-space vector is available [9]. Since the logical basis of this method has already been spelt out in detail [9], only the main steps in the implementation of the algorithm will be outlined here.

We begin by defining the two-component vectors

$$\mathbf{J}_q \triangleq \left[ \hat{J}_{zq}, \hat{J}_{\varphi q} \right]^T, \quad -N \leq q \leq N$$

and the  $2 \times 2$  matrices

$$\mathbf{a}_{kq} = \begin{bmatrix} b_{kq} & -c_{kq} \\ c_{kq} & -d_{kq} \end{bmatrix}, \quad -N \leq k, q \leq N$$

### (i) Iterative computation of matrix coefficients

*Initialization:*  $\mathbf{a}_{kl}^{(0)} \equiv \mathbf{a}_{kl}, \quad -N \leq k, l \leq N$

*Recursion:*

$$\mathbf{a}_{N-i, N-i}^{(i)} = \mathbf{a}_{N-i, N-i}^{(i-1)} - \mathbf{a}_{N-i, N-i+1}^{(i-1)} \left( \mathbf{a}_{N-i+1, N-i+1}^{(i-1)} \right)^{-1} \mathbf{a}_{N-i+1, N-i}^{(i-1)}$$

for  $1 \leq i \leq N - 1$ ,

$$\mathbf{a}_{N-i, N-i-1}^{(i)} = \mathbf{a}_{N-i, N-i-1} - \mathbf{a}_{N-i, N-i+1}^{(i-1)} \left( \mathbf{a}_{N-i+1, N-i+1}^{(i-1)} \right)^{-1} \mathbf{a}_{N-i+1, N-i-1}$$

for  $1 \leq i \leq N - 1$ ,

$$\mathbf{a}_{N-i-1, N-i}^{(i)} = \mathbf{a}_{N-i-1, N-i} - \mathbf{a}_{N-i-1, N-i+1} \left( \mathbf{a}_{N-i+1, N-i+1}^{(i-1)} \right)^{-1} \mathbf{a}_{N-i+1, N-i}^{(i-1)}$$

for  $1 \leq i \leq N - 1$ ,

$$\begin{aligned}
\mathbf{a}_{N-i-1, N-i-1}^{(i)} &= \mathbf{a}_{N-i-1, N-i-1} \\
&\quad - \mathbf{a}_{N-i-1, N-i+1} \left( \mathbf{a}_{N-i+1, N-i+1}^{(i-1)} \right)^{-1} \mathbf{a}_{N-i+1, N-i-1} \\
&\hspace{20em} \text{for } 1 \leq i \leq N-2,
\end{aligned} \tag{13}$$

together with a corresponding set of relations with an overbar over the suffixes.

$$\begin{aligned}
\mathbf{a}_{10}^{(N)} &= \left[ \left( \mathbf{a}_{\bar{1}\bar{1}}^{(N-1)} \right)^{-1} \mathbf{a}_{\bar{1}\bar{1}} - \mathbf{a}_{\bar{1}\bar{1}}^{-1} \mathbf{a}_{\bar{1}\bar{1}}^{(N-1)} \right]^{-1} \\
&\quad \times \left[ \mathbf{a}_{\bar{1}\bar{1}}^{-1} \mathbf{a}_{10}^{(N-1)} - \left( \mathbf{a}_{\bar{1}\bar{1}}^{(N-1)} \right)^{-1} \mathbf{a}_{\bar{1}\bar{1}}^{(N-1)} \right]
\end{aligned} \tag{14}$$

and the relation for  $\mathbf{a}_{10}^{(N)}$  is derived from (12) by complementing all suffixes where  $\bar{1}\bar{1}\triangle 1$  and  $\bar{0}\bar{0}\triangle 0$ .

Finally

$$\begin{aligned}
\mathbf{a}_{00}^{(N)} &= \mathbf{a}_{00} + \mathbf{a}_{0\bar{1}}^{(N-1)} \mathbf{a}_{10}^{(N)} + \mathbf{a}_{01}^{(N-1)} \mathbf{a}_{10}^{(N)} \\
&\quad - \mathbf{a}_{0\bar{2}} \left( \mathbf{a}_{\bar{2}\bar{2}}^{(N-2)} \right)^{-1} \mathbf{a}_{\bar{2}0} - \mathbf{a}_{02} \left( \mathbf{a}_{22}^{(N-2)} \right)^{-1} \mathbf{a}_{20}
\end{aligned} \tag{15}$$

## (ii) Iterative computation of the current-density coefficients

Let  $\lambda_{kl}^{(N)}$ ,  $k, l = 1, 2$ , be the entries of the rank-one  $2 \times 2$  matrix  $\mathbf{a}_{00}^{(N)}$ . Set

$$\hat{\lambda}_N(k_{0a}) \triangleq \lambda_N(\hat{\beta}_{0a}(k_{0a})) = -\lambda_{12}^{(N)} / \lambda_{11}^{(N)} = -\lambda_{22}^{(N)} / \lambda_{21}^{(N)}$$

*Initialization:*

$$\hat{\mathbf{J}}_0 = [\hat{\lambda}_N(k_{0a}), 1]^T \hat{J}_{\varphi 0}, \tag{16}$$

where  $\hat{J}_{\varphi 0}$  is an undetermined (complex) constant.

*Recursion:*

$$\hat{\mathbf{J}}_1 = \mathbf{a}_{10}^{(N)} \hat{\mathbf{J}}_0 \quad \text{and} \quad \hat{\mathbf{J}}_{\bar{1}} = \mathbf{a}_{\bar{1}0}^{(N)} \hat{\mathbf{J}}_0 \tag{17}$$

$$\begin{aligned}
\hat{\mathbf{J}}_{N-i} &= - \left( \mathbf{a}_{N-i, N-i}^{(i)} \right)^{-1} \left[ \mathbf{a}_{N-i, N-i-1}^{(i)} \hat{\mathbf{J}}_{N-i-1} + \mathbf{a}_{N-i, N-i-2} \hat{\mathbf{J}}_{N-i-2} \right] \\
&\hspace{15em} \text{for } 0 \leq i \leq N-2
\end{aligned} \tag{18}$$

together with a corresponding set of relations with an overbar over the suffixes.

**(iii) Computation of the tape-current distribution**

The coefficients  $\hat{J}_{||n}$  and  $\hat{J}_{\perp n}$  for  $-N \leq n \leq N$  of the surface current density components  $\hat{J}_{||}(z, \zeta) = e^{-j\beta_{0z}} \hat{f}_{||}(\zeta)$  and  $\hat{J}_{\perp}(z, \zeta) = e^{-j\beta_{0z}} \hat{f}_{\perp}(\zeta)$  parallel and perpendicular to the winding direction are obtained in terms of the current-density coefficients  $\hat{J}_{zn}$  and  $\hat{J}_{\varphi n}$ ,  $-N \leq n \leq N$  as

$$\begin{bmatrix} \hat{J}_{||n} \\ \hat{J}_{\perp n} \end{bmatrix} = \begin{bmatrix} \sin \psi & \cos \psi \\ \cos \psi & -\sin \psi \end{bmatrix} \begin{bmatrix} \hat{J}_{zn} \\ \hat{J}_{\varphi n} \end{bmatrix}, \quad -N \leq n \leq N,$$

where

$$\hat{f}_{||}(\zeta) = \sum_{n=-N}^N \hat{J}_{||n} e^{-j2\pi n\zeta/p}, \quad -p/4 \leq \zeta \leq p/4,$$

and  $\hat{f}_{\perp}(\zeta) = \sum_{n=-N}^N \hat{J}_{\perp n} e^{-j2\pi n\zeta/p}, \quad -p/4 \leq \zeta \leq p/4,$

are the truncated Fourier series of the restrictions of the periodic functions

$$\sum_{l=-\infty}^{\infty} 1_{[lp-w/2, lp+w/2]}(\zeta) \sum_{n=-N}^N \hat{J}_{||n} e^{-j2\pi n\zeta/p}$$

and  $\sum_{l=-\infty}^{\infty} 1_{[lp-w/2, lp+w/2]}(\zeta) \sum_{n=-N}^N \hat{J}_{\perp n} e^{-j2\pi n\zeta/p}$

of period  $p$  to the interval  $[-p/4, p/4]$ . We may now define normalized surface current density components parallel and perpendicular to the winding direction as

$$\hat{I}_{||}(\zeta) = \left| \hat{I}_{||}(\zeta) \right| e^{j\varphi_{||}(\zeta)} \triangleq \hat{J}_{||}(z, \zeta) / \hat{J}_{||}(z, 0) = \hat{f}_{||}(\zeta) / \hat{f}_{||}(0)$$

and  $\hat{I}_{\perp}(\zeta) = \left| \hat{I}_{\perp}(\zeta) \right| e^{j\varphi_{\perp}(\zeta)} \triangleq \hat{J}_{\perp}(z, \zeta) / \hat{J}_{\perp}(z, 0) = \hat{f}_{\perp}(\zeta) / \hat{f}_{\perp}(0)$

The magnitude and the phase of the normalized surface density components  $\hat{I}_{||}(\zeta)$  and  $\hat{I}_{\perp}(\zeta)$  are computed for the choice of values 3, 8 and 14.25 of the normalized propagation constant  $\beta_{0a}$  corresponding to the first, the second and the third allowed region in the  $k_{0a} - \beta_{0a}$  plane for a truncation order  $N = 80$ . The roots of the dispersion equation for  $\hat{k}_{0a}(\beta_{0a})$  corresponding to the above three values of  $\beta_{0a}$  are 0.52215, 1.39015 and 2.43885 respectively. The variation of the magnitude and the phase of the normalized surface current density components  $\hat{I}_{||}(\zeta)$  and  $\hat{I}_{\perp}(\zeta)$  with respect to  $\zeta/p$  are plotted in Figs. 2–4.

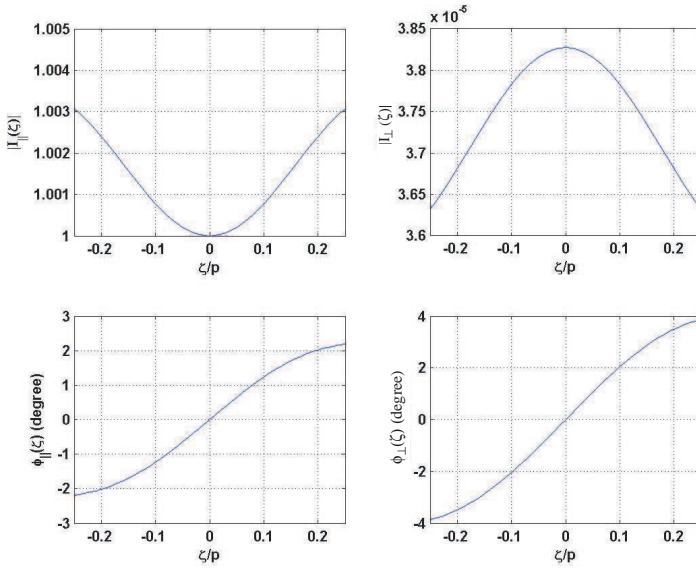


**Figure 2.** Distribution of surface current density components for  $\beta_{0a} = 3$ .

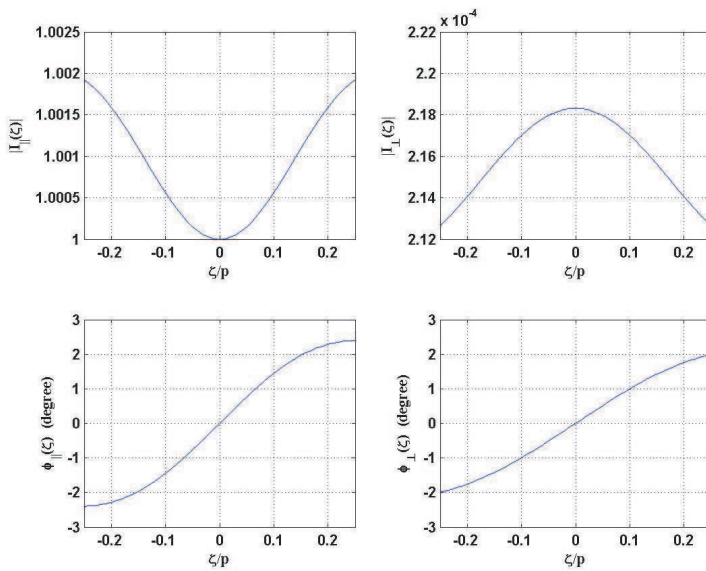


**Figure 3.** Distribution of surface current density components for  $\beta_{0a} = 8$ .

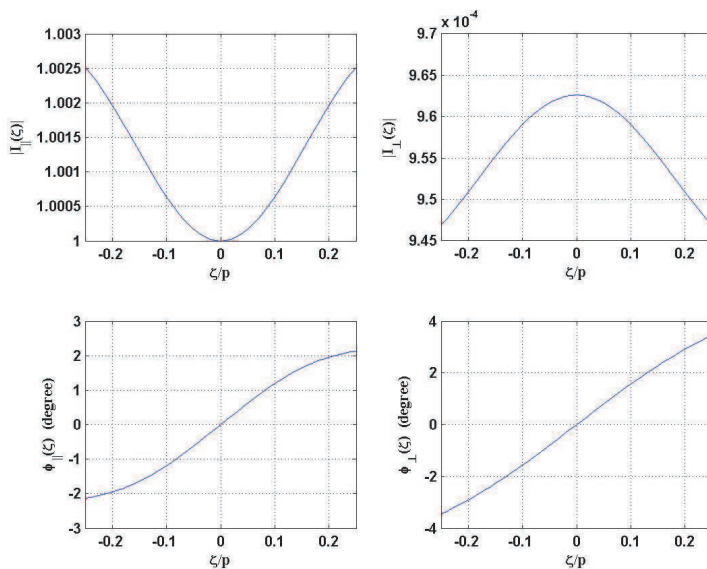


**Figure 4.** Distribution of surface current density components for  $\beta_{0a} = 14.25$ .

#### 4. DISCUSSION AND CONCLUSIONS

The following conclusions may be drawn from the plots of Figs. 2–4: (i) The magnitude and the phase of the current distribution on the tape surface are nearly uniform at all frequencies falling within the allowed regions even for tapes which are not narrow. (ii) The magnitude of the surface current density component perpendicular to the winding direction is at least three orders of magnitude smaller than that parallel to the winding direction for all  $\zeta \in [-p/4, p/4]$ . (iii) The ratio  $|\hat{I}_\perp(\zeta)/\hat{I}_\parallel(\zeta)|$  of the current density component magnitudes tends to increase with an increase in the frequency. (iv) None of the surface current density components exhibits any singular behavior near the tape edges; however, since the current density is seen to drop discontinuously to zero beyond the tape edges, the continuity equation implies that the surface charge density will be singular at the tape edges. This nonphysical situation leading to the discontinuity of the surface current density at the tape edges arises out of our assumption of an infinitesimally thin tape. In the realistic case of a tape of finite thickness and rounded edges, the continuity of current, which

is confined essentially to a thin layer adjacent to the tape surface, will be maintained across the tape edges and there will not be any discontinuity in the current flow. However, the development of an adequate model for a tape of finite thickness that is amenable to an exact analysis still remains as a challenging open problem.

The observation made in the last paragraph regarding the relative magnitudes of the two current-density components makes the anisotropically conducting model of the tape helix that neglects the perpendicularly directed component of the surface current density appear quite plausible. Unfortunately, such a model that has been in vogue for not less than five decades for narrow tapes turns out to be mathematically ill-posed for the following reason: The coefficients  $\hat{J}_n$ ,  $n \in \mathbb{Z}$ , of the tape current density expansion computed on the basis of an exact analysis of the anisotropically conducting model [10] tends to grow in magnitude with  $|n|$ . This undesirable asymptotic behavior of the current-density coefficients is directly linked to the asymptotic behavior of the  $\sigma_n$ ,  $n \in \mathbb{Z}$ , (Please refer to (46) of [10] for the definition) which tends to decay in magnitude with respect to  $|n|$ . In contrast, the analogous parameters  $\mu_n, \nu_n$  and  $\eta_n$ ,  $n \in \mathbb{Z}$ , featuring in the perfectly conducting tape-helix model being made use of in this paper tend to grow linearly with  $|n|$ . Since the current-density coefficients  $\hat{J}_n$ ,  $n \in \mathbb{Z}$ , appearing in [10], serve as the Fourier coefficients in a Fourier-series expansion of the tape-current density and since the Fourier coefficients of any periodic function that is absolutely integrable ( $L^1$ ) over a period must tend to zero as  $|n| \rightarrow \infty$  in accordance with Riemann-Lebesgue lemma [11], the inescapable inference is that a model of the tape helix that neglects the perpendicularly directed component of the tape current density is not capable of leading to a well-posed mathematical problem.

## REFERENCES

1. Sensiper, S., "Electromagnetic wave propagation on helical conductors," Sc.D. Thesis, Massachusetts Institute of Technology, Cambridge, Mar. 1951.
2. Chodorov, M. and E. L. Chu, "Cross-wound twin helices for traveling-wave tubes," *J. Appl. Phys.*, Vol. 26, No. 1, 33–43, 1955.
3. Watkins, D. A., *Topics in Electromagnetic Theory*, John Wiley & Sons, New York, 1958.
4. Zhang, K. A. and D. Li, *Electromagnetic Theory for Microwaves and Optoelectronics*, 2nd edition, Springer-Verlag, Berlin-Heidelberg, 2008.

5. Basu, B. N., *Electromagnetic Theory and Applications in Beam-wave Electronics*, World Scientific, Singapore, 1996.
6. D'Agostino, S., F. Emma, and C. Paoloni, "Accurate analysis of helix slow-wave structures," *IEEE Trans. Electron Devices*, Vol. 45, No. 7, 1605–1613, 1998.
7. Tsutaki, K., Y. Yuasa, and Y. Morizumi, "Numerical analysis and design for high-performance helix traveling wave tubes," *IEEE Trans. Electron Devices*, Vol. 32, No. 9, 1842–1849, 1985.
8. Chernin, D., T. M. Antonsen, and B. Levush, "Exact treatment of the dispersion and beam interaction impedance of a thin tape helix surrounded by a radially stratified dielectric," *IEEE Trans. Electron Devices*, Vol. 46, No. 7, 1472–1483, 1999.
9. Kalyanasundaram, N. and G. Naveen Babu, "Dispersion of electromagnetic waves guided by an open tape helix II," *Progress In Electromagnetic Research B*, Vol. 19, 133–150, 2010.
10. Kalyanasundaram, N. and G. Naveen Babu, "Dispersion of electromagnetic waves guided by an open tape helix I," *Progress In Electromagnetic Research B*, Vol.16, 311–331, 2009.
11. Katznelson, Y., *An Introduction to Harmonic Analysis*, 3rd edition, Cambridge University Press, 2004.